

Physics Performance of a Low-Luminosity Low Energy Neutrino Factory

E. Christensen,¹ P. Coloma,¹ and P. Huber¹

¹*Center for Neutrino Physics, Virginia Tech, Blacksburg, VA 24061, USA*

(Dated: February 1, 2013)

We investigate the minimal performance, in terms of beam luminosity and detector size, of a neutrino factory to achieve a competitive physics reach for the determination of the mass hierarchy and the discovery of leptonic CP violation. We find that a low luminosity of 10^{20} useful muon decays per year and 5 GeV muon energy aimed at a 10 kton magnetized liquid argon detector placed at 1300 km from the source provides a good starting point. This result relies on θ_{13} being large and assumes that the so-called platinum channel can be used effectively. We find that such a minimal facility would perform significantly better than phase I of the LBNE project and thus could constitute a reasonable step towards a full neutrino factory.

PACS numbers: 14.60.Pq, 14.60.Lm

Keywords: neutrino oscillation, neutrino mixing, CP violation

The recent discovery of θ_{13} is a major step towards the completion of the leptonic mixing matrix. The first hints in global fits soon were followed by T2K [1], MINOS [2] and Double-Chooz [3], and by now Daya Bay, RENO and Double-Chooz have observed this parameter at 7.7σ , 4.9σ and 2.9σ , respectively [4–6]. The remaining major unknowns in the lepton sector are the Dirac CP violating phase, δ and the ordering of the neutrino mass eigenstates, $\text{sgn}(\Delta m_{31}^2)$. The large value of θ_{13} admits many methods to determine the mass hierarchy (MH), some of which do not rely on long-baseline oscillation experiments, and therefore, we mostly will focus on the measurement of the CP phase.

In order to measure CP violation (CPV), an appearance experiment and consequently, a neutrino beam, is mandatory. The combination of T2K [7] and NO ν A [8] may provide a hint for CPV, but the possibilities to obtain evidence at the 3σ level are rather limited [9]. Therefore a next generation neutrino beam is needed.

A multitude of experiments has been proposed in order to observe CPV in the leptonic sector, see for instance Ref. [10]. In the U.S. context, the long baseline neutrino experiment (LBNE) is the currently preferred option. The present design consists of a 700 kW conventional neutrino beam aimed at a 10 kton liquid argon (LAr) detector placed at $L = 1300$ km from the source [11]. Due to its long baseline and relatively large matter effects, LBNE would be able to determine the MH at 3σ for a 75% of the parameter space. The CPV discovery potential is, however, limited due to a lack of statistics. An upgraded superbeam would obviously yield a much better physics potential [12]. However, superbeams are eventually limited by intrinsic backgrounds and systematic effects: the large flux uncertainties, combined with the inability to measure the

final flavor cross sections at the near detector, introduce large systematical errors [13, 14] which are very difficult to control.

For the determination of the CP phase a similar precision to that achieved in the quark sector is only offered by a neutrino factory (NF) [14, 15]. In a NF a highly collimated beam of muon neutrinos and electron antineutrinos is produced from muon decays in a storage ring with long straight sections [16]. The muons stem from pion decays and the pions, in turn, are produced by proton irradiation of a thick target. The present NF design parameters [17] are 10^{21} useful muon decays per 10^7 seconds, aimed to a 100 kton magnetized iron detector (MIND) placed at 2000 km from the source, with a parent muon muon energy of 10 GeV. In order to form an intense muon beam for acceleration and storage, muon phase space cooling is required for this default configuration. In addition, the fact that the neutrinos in a NF are a tertiary beam implies significant proton driver intensities; in this case, a 4 MW proton beam plus its associated target station. Thus, the challenges for an early implementation of a NF are clear: high proton beam power and muon cooling.

These technical challenges are to be contrasted with the advantages of a NF – there are no intrinsic backgrounds and the absolute neutrino flux can be determined to much better than 1%. Furthermore, the presence of both muon and electron neutrinos in the beam does allow for a measurement of all final flavor cross sections at the near detector. A detailed analysis of the impact of systematic uncertainties in neutrino oscillation experiments has been recently performed in Ref. [14], where the key systematics affecting the different types of facilities were identified. In particular, it was shown that the main sources of systematics affecting a NF are matter density uncertainties (see also Ref. [18]). On the

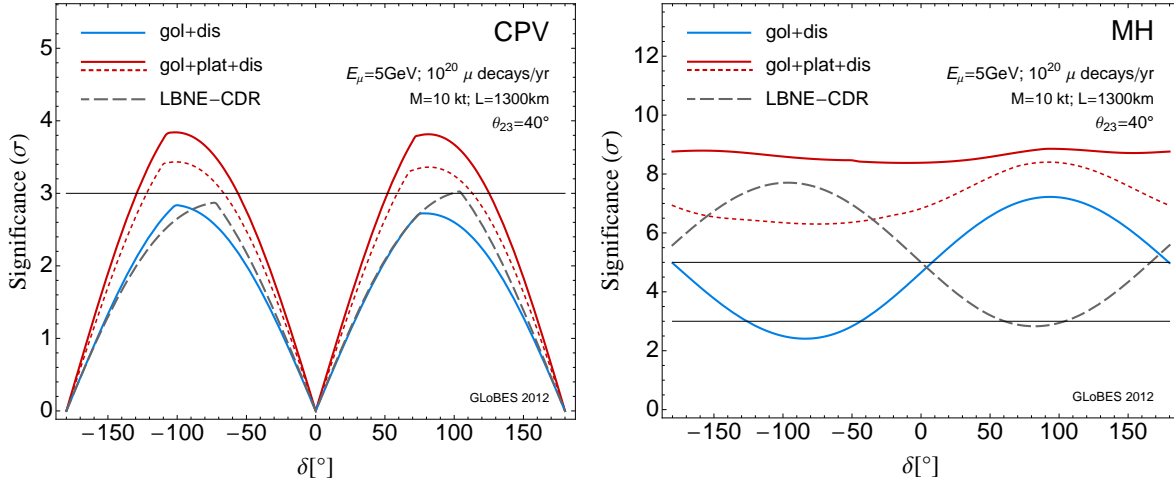


FIG. 1: CP violation (left panel) and mass hierarchy (right panel) discovery potentials. The statistical significance (for 1 d.o.f.) is shown as a function of the true value of δ , in the case when only the golden and disappearance channels are included in the analysis (blue lines, “gol+dis”), as well as when the platinum channel is also considered (red lines, “gol+dis+plat”). Dotted red lines show the results for the TASD detector, while solid lines refer to LAr. For reference, the results for the preferred reconfiguration option for LBNE are also shown (dashed gray lines).

other hand, it was shown in Ref. [19] that, for a large value of θ_{13} , the use of the so-called platinum channel, $\nu_\mu \rightarrow \nu_e$ and $\bar{\nu}_\mu \rightarrow \bar{\nu}_e$, mitigates the effects from the matter density uncertainty. However, the platinum channel is inaccessible in a MIND, because it requires to identify electron neutrino charged current events. The feasibility of electron charge identification was studied in Ref. [20] in the context of a low energy NF for a totally active scintillator detector (TASD) magnetized to 0.5 T using a so-called magnetic cavern. It soon was speculated that a magnetized LAr detector should be suitable as well [21–23]. Note, that the detectors most likely will have to be deep underground due to the large duty factor of stored particle beams as in a NF.

Specifically, we study a configuration with a muon energy of 5 GeV, 10^{20} useful muon decays per year and polarity and a 10 kt magnetized LAr detector at a distance of 1300 km. This choice of detector size and baseline is obviously inspired by LBNE: it allows to reuse the LBNE facilities to the largest possible extent and thus makes this option considerably more efficient in terms of resource usage. These parameters correspond to an overall reduction in exposure by a factor 100, and would in principle allow the NF to be based entirely on existing infrastructure and technology. To give a specific example – the reduced beam luminosity would allow to use the *existing* Fermilab proton beam from the Main Injector with a beam power of 700 kW and a beam energy of 60-120 GeV. This would result in a reduction of

luminosity by a factor 10 with respect to the default setup [17] – a factor ~ 5 from the beam power and factor 2 from the reduced pion production efficiency at higher beam energy. Furthermore, giving up muon cooling would result in the loss of another factor of 2 in luminosity. Conversely, an increase in the annual operation time from 10^7 s to 2×10^7 s, commonly used for Fermilab experiments, would result in a gain of a factor of 2. As a result we finally obtain the postulated 10^{20} useful muon decays per polarity and year. This is but one example of how to achieve this entry level luminosity. Obviously, future proton beam facilities may have much more favorable parameters resulting in corresponding increases in luminosity.

Tab. I summarizes the detector parameters used in this work. A magnetized detector is required at a NF in order to disentangle the appearance and disappearance signals. In the absence of a detailed study of the performance of a magnetized LAr detector, we have followed Refs. [12, 22]. Since the LAr performance is indeed uncertain, we also evaluate sensitivities using the performance parameters of a TASD, which have been studied in greater detail [20]. The same migration matrices and energy resolution as for the LAr detector have been considered. Energy dependent efficiencies for the signal, following Ref. [22], have been used in this case, see Tab. I. As for the backgrounds, we have considered the same rejection capabilities as for the LAr for muon detection, while for the electron detection we

have considered 10 times larger backgrounds. Finally, ^{40}Ar cross sections have been used in both cases, which have been generated using GENIE [24].

In addition to the backgrounds considered in previous references, the τ -contamination [25–27] has also been included in this work. In this case, no rejection capability at all is considered when the polarity and flavor of the lepton produced in the τ -decay is the same as that of the signal; while when the polarity is the opposite a 99.9% background rejection has been assumed. Migration matrices, which account for the kinematics of the τ -decay and the mis-reconstruction of the events at lower energies, have been generated using GENIE. A 17% τ leptonic branching ratio has been assumed in all cases.

Channel	Effs.	Bg. Rej.	$\sigma(E_\nu)$	E_ν (GeV)
LAr	ν_μ	80%	99.9%	$0.2\sqrt{E}$ [0.5, 5]
	ν_e	80%	99.9%	$0.15\sqrt{E}$ [0.5, 5]
TASD	ν_μ	73%-94%	99.9%	$0.2\sqrt{E}$ [0.5, 5]
	ν_e	37%-47%	99%	$0.15\sqrt{E}$ [0.5, 5]

TABLE I: Main details used to simulate the LAr and TASD detector responses. The two rows correspond to the details used for ν_μ and ν_e detection. The different columns indicate: signal efficiencies, background rejection efficiencies (Neutral Current, Charge misID, Flavor misID), energy resolution and neutrino energy range. NC backgrounds have been migrated to lower energies using migration matrices produced by the LBNE collaboration [12]. For details on the implementation of the τ -contamination, see main text.

Systematic uncertainties have been implemented as in Ref. [14], using the default values for the systematic uncertainties listed in Tab. 2 therein. The only new systematic uncertainty introduced in this work is the one associated to ν_τ cross sections, for which we have (conservatively) assumed a 45% uncertainty. All correlations are taken into account, between different channels as well as between the near and far detectors. All simulations have been done using a modification of GLOBES [28, 29], and marginalization over not-shown oscillation parameters was performed as explained in Ref. [14].

Figure 1 shows the results for the CPV and MH discovery potentials of the facility. These are defined as the ability of the experiment to rule out the CP conservation hypothesis and the wrong mass hierarchy, respectively, and their statistical significance is shown as a function of the true value of δ . For reference, we also show the results for phase

I of the LBNE experiment, which has been simulated according to the CDR from October 2012, Ref. [11]. Therefore, no τ -contamination has been included in this case, and systematic uncertainties have been implemented as overall normalization errors over all signal and background contributions at once (no near detector has been simulated for this setup). Clearly, the low energy, low luminosity NF outperforms LBNE by a considerable margin once the platinum channel is included.

The left panel in Fig. 2 shows the allowed region in θ_{13} - δ plane for one particular point in the parameter space, where the different line styles correspond to different combinations of channels and/or experiments. Clearly, the addition of the platinum channel improves the performance beyond a mere increase of statistics – a true synergy, whose origin is explained in Ref. [19]. The right hand panel, on the other hand, shows the achievable precision for a measurement of δ at 1σ as a function of the true value of δ . Again, we find that the low luminosity low energy NF constitutes a marked improvement over LBNE.

We also would like to point out, that once a 4 MW lower energy proton beam becomes available from Project X, muon cooling is added and the detector mass is increased by a factor 1-3, the performance of this facility matches or even exceeds the one of the baseline NF. Therefore, neither the initial energy of 5 GeV nor the baseline do need to be changed in later stages.

In summary, using 10 times less useful muon decays and a 10 times smaller detector mass with respect to the baseline NF still allows a muon decay based neutrino beam to outperform realistic superbeam setups like LBNE, while offering at the same time the path to a full scale NF. Such low luminosity can be achieved using existing proton drivers and without muon cooling. Therefore, the timescale for an experiment like this would in principle be comparable to that of a superbeam experiment. Consequently, it lends itself well as an option for a second phase of an initial superbeam experiment. The reduced muon energy makes it possible to use a shorter baseline around 1300 km, and the use of a magnetized LAr detector allows to fully exploit the physics potential of the platinum channel, which is crucial for the overall performance of the facility. At the same time, these choice for baseline and detector technology ensure a good synergy with the first stage of a superbeam program. The big open question is how well can a LAr detector perform this task.

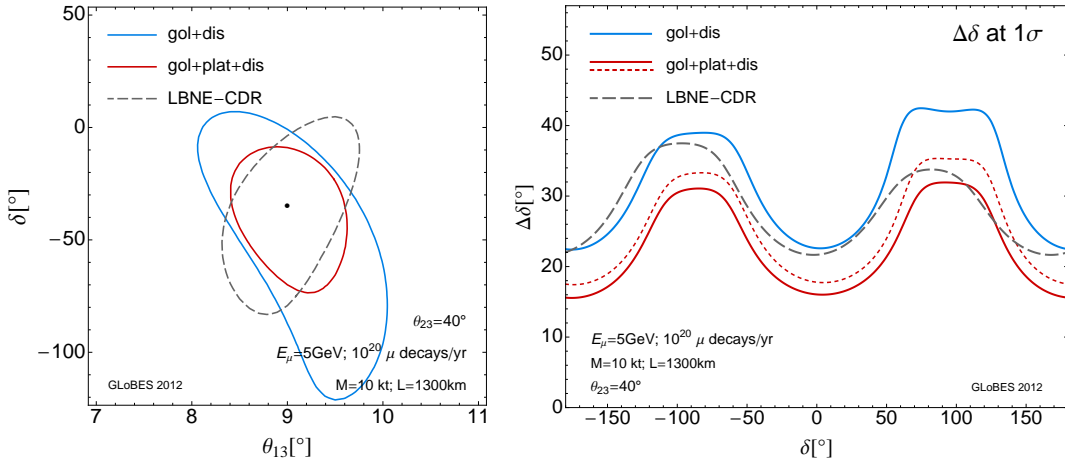


FIG. 2: Left panel: confidence region in the $\theta_{13} - \delta$ plane for a particular point in the parameter space, at 1σ CL (2 d.o.f.). Right panel: precision achievable for a measurement in δ at the 1σ CL (1 d.o.f.), as a function of the true value of δ . Results are shown when only the golden and disappearance channels are included in the analysis (blue lines, “gol+dis”), as well as when the platinum channel is also considered (red lines, “gol+dis+plat”). Dotted red lines show the results for a TASD detector, while solid lines refer to LAr. For reference, the results for the preferred reconfiguration option for LBNE are also shown (dashed gray lines).

This work has been supported by the U.S. Department of Energy under award number DE-SC0003915. We would like to thank M. Bishai and M. Bass for helping us to reproduce the LBNE sensitivities.

-
- [1] K. Abe et al. (T2K Collaboration), Phys.Rev.Lett. **107**, 041801 (2011), 1106.2822.
 - [2] P. Adamson et al. (MINOS Collaboration), Phys.Rev.Lett. **107**, 181802 (2011), 1108.0015.
 - [3] Y. Abe et al. (DOUBLE-CHOOZ Collaboration), Phys.Rev.Lett. **108**, 131801 (2012), 1112.6353.
 - [4] F. An et al. (Daya Bay Collaboration) (2012), 1210.6327.
 - [5] J. Ahn et al. (RENO collaboration), Phys.Rev.Lett. **108**, 191802 (2012), 1204.0626.
 - [6] Y. Abe et al. (Double Chooz Collaboration), Phys.Rev. **D86**, 052008 (2012), 1207.6632.
 - [7] Y. Itow et al. (The T2K Collaboration), pp. 239–248 (2001), hep-ex/0106019.
 - [8] D. Ayres et al. (NOvA Collaboration) (2007).
 - [9] P. Huber, M. Lindner, T. Schwetz, and W. Winter, JHEP **0911**, 044 (2009), 0907.1896.
 - [10] S. Agarwalla, E. Akhmedov, M. Blennow, P. Coloma, A. Donini, et al. (2012), 1209.2825.
 - [11] LBNE Conceptual Design Report from Oct 2012, volume 1, URL <http://lbne.fnal.gov/papers.shtml>.
 - [12] T. Akiri et al. (LBNE Collaboration) (2011), 1110.6249.
 - [13] P. Huber, M. Mezzetto, and T. Schwetz, JHEP **0803**, 021 (2008), 0711.2950.
 - [14] P. Coloma, P. Huber, J. Kopp, and W. Winter

- (2012), 1209.5973.
- [15] P. Coloma, A. Donini, E. Fernandez-Martinez, and P. Hernandez, JHEP **1206**, 073 (2012), 1203.5651.
- [16] S. Geer, Phys.Rev. **D57**, 6989 (1998), hep-ph/9712290.
- [17] S. Choubey et al. (IDS-NF Collaboration) (2011), 1112.2853.
- [18] P. Huber, M. Lindner, and W. Winter, Nucl.Phys. **B645**, 3 (2002), hep-ph/0204352.
- [19] P. Huber, M. Lindner, M. Rolinec, and W. Winter, Phys.Rev. **D74**, 073003 (2006), hep-ph/0606119.
- [20] A. D. Bross, M. Ellis, S. Geer, O. Mena, and S. Pascoli, Phys.Rev. **D77**, 093012 (2008), 0709.3889.
- [21] P. Kyberd, M. Ellis, A. Bross, S. Geer, O. Mena, et al. (2009).
- [22] E. Fernandez Martinez, T. Li, S. Pascoli, and O. Mena, Phys.Rev. **D81**, 073010 (2010), 0911.3776.
- [23] P. Ballett and S. Pascoli, Phys.Rev. **D86**, 053002 (2012), 1201.6299.
- [24] C. Andreopoulos, A. Bell, D. Bhattacharya, F. Cava, J. Dobson, et al., Nucl.Instrum.Meth. **A614**, 87 (2010), 0905.2517.
- [25] D. Indumathi and N. Sinha, Phys.Rev. **D80**, 113012 (2009), 0910.2020.
- [26] A. Donini, J. Gomez Cadenas, and D. Meloni, JHEP **1102**, 095 (2011), 1005.2275.
- [27] R. Dutta, D. Indumathi, and N. Sinha, Phys.Rev. **D85**, 013003 (2012), 1103.5578.
- [28] P. Huber, M. Lindner, and W. Winter, Comput.Phys.Commun. **167**, 195 (2005), hep-ph/0407333.
- [29] P. Huber, J. Kopp, M. Lindner, M. Rolinec, and W. Winter, Comput.Phys.Commun. **177**, 432 (2007), hep-ph/0701187.